Solid State Communications 273 (2018) 23–29

Contents lists available at ScienceDirect

Solid State Communications

journal homepage: www.elsevier.com/locate/ssc

Communication

Theoretical simulations of the structural stabilities, elastic, thermodynamic and electronic properties of Pt_3Sc and Pt_3Y compounds

R. Boulechfar [a,b], Y. Khenioui [a], S. Drablia [b], H. Meradji [b,*], M. Abu-Jafar [c], S. Bin Omran [d], R. Khenata [e], S. Ghemid [b]

[a] Département de Technologie, Faculté de Technologie, Université du 20 Août 1955-Skikda, Algeria
[b] Laboratoire LPR, Département de Physique, Faculté des Sciences, Université de Annaba, Algeria
[c] Physics Department, An Najah National University, Nablus, Palestine
[d] Department of Physics and Astronomy, College of Science, King Saud University, P.O. Box 2455, Riyadh 11451, Saudi Arabia
[e] Laboratoire de Physique Quantique de la Matière et de la Modélisation Mathématique (LPQ3M), Université de Mascara, Mascara 29000, Algeria

ARTICLE INFO

Communicated Editor: J. R. Chelikowsky

Keywords:
A. Intermetallic
D. Ductile
Pseudo-gap
E. FP-LAPW
C. $L1_2$

ABSTRACT

Ab-initio calculations based on density functional theory have been performed to study the structural, electronic, thermodynamic and mechanical properties of intermetallic compounds Pt_3Sc and Pt_3Y using the full-potential linearized augmented plane wave(FP-LAPW) method. The total energy calculations performed for $L1_2$, $D0_{22}$ and $D0_{24}$ structures confirm the experimental phase stability. Using the generalized gradient approximation (GGA), the values of enthalpies formation are −1.23 eV/atom and −1.18 eV/atom for Pt_3Sc and Pt_3Y, respectively. The densities of states (DOS) spectra show the existence of a pseudo-gap at the Fermi level for both compounds which indicate the strong *spd* hybridization and directing covalent bonding. Furthermore, the density of states at the Fermi level $N(E_F)$, the electronic specific heat coefficient (γ_{ele}) and the number of bonding electrons per atom are predicted in addition to the elastic constants (C_{11}, C_{12} and C_{44}). The shear modulus (G_H), Young's modulus (E), Poisson's ratio (ν), anisotropy factor (A), ratio of B/G_H and Cauchy pressure (C_{12}–C_{44}) are also estimated. These parameters show that the Pt_3Sc and Pt_3Y are ductile compounds. The thermodynamic properties were calculated using the quasi-harmonic Debye model to account for their lattice vibrations. In addition, the influence of the temperature and pressure was analyzed on the heat capacities (C_p and C_v), thermal expansion coefficient (α), Debye temperature (θ_D) and Grüneisen parameter (γ).

1. Introduction

Recently, the platinum alloys have known a growing role and demand in a large variety of industrial applications. They find their use as a major constituent in automotive, jewelry and other areas of industry. Pt-based intermetallic compounds exhibit many attractive properties, making them promising candidates in material science and engineering. Their properties include mainly low density, high melting point and resistance to oxidation and corrosion. However, the lack of ductility at room temperature limits their use as structural applications [1–4]. Pt-alloys with early transition metals are considered as promising in the oxygen reduction reaction (ORR) [5–7] due to their highly negative enthalpy of formation [8,9]. In this paper, we mainly focus on the physical and mechanical properties of some of these alloys, i.e., Pt_3Sc and Pt_3Y compounds. The experimental measurements show that both compounds crystallize in the cubic $L1_2$ structure [10,11]. In the intermetallic compounds studies, the $L1_2$ crystal structure have a large number of slip systems which increase the ductility of these compounds compared to tetragonal structures $D0_{22}$, $D0_{23}$, $D0_{24}$ … etc. There have been considerable works involving both experimental and theoretical methods on $L1_2$intermetallic compounds. Razumovskiy et al. [12] investigated the elastic properties of substitutionally disordered Pt–Sc alloys and $L1_2$-ordered Pt_3Sc compound using first-principles calculations based on the exact muffin-tin orbitals (EMTO) method. Goncharuk and co-workers performed EMF measurement for galvanic cells used in the range 813–1023 K and measured the Gibbs energies, enthalpies and entropies of formation of ScIr3 [13]. Arikan and co-authors studied the structural, elastic, electronic and phonon properties of scandium-based compound ScX_3 (X = Ir, Pd, Pt and Rh) by employing the self-consistent pseudopotential method [14]. Chen and co-authors investigated the structural, elastic, electronic and thermodynamic

* Corresponding author. Tel.: +213 7 79 27 82 21
E-mail address: hmeradji@yahoo.fr (H. Meradji).

https://doi.org/10.1016/j.ssc.2018.02.005
Received 19 September 2017; Received in revised form 22 January 2018; Accepted 7 February 2018
Available online 9 February 2018

properties of ScX_3 (X = Ir, Pd, Pt and Rh) compounds under high pressure by using the ab initio pseudo potential method implemented in CASTEP code [15]. The structural and electronic properties of ScRh3 have been studied by Giannozzi et al. [16] and Sundareswari and M. Rajagopalan [17] using the ab initio pseudo potential method integrated in Vienna package code and the tight binding linear muffin-tin orbitals (TB-LMTO) method, respectively. Jeong studied the electronic properties of ScPd3 by employing the full-potential non orthogonal local orbital minimum-basis (FPLO) scheme within the local density approximation (LDA) [18]. From the above, it is clear that there are no reported experimental data in the literature on the elastic constants and the thermodynamic properties for the $ScPt_3$. Neither experimental nor theoretical details regarding the elastic, electronic and thermodynamic properties of ScY_3 are available. Moreover, all the theoretical calculations devoted to these compounds are not full potential calculations. These reasons motivate us to perform these calculations in order to provide another reference data for the exciting theoretical works on this fascinating class of materials, using the full-potential linear augmented plane-wave (FP-LAPW) method within the density functional theory (DFT), which has proven to be one of the most accurate methods [19,20] for the computation of the electronic structure of solids.

The rest of the paper is divided into three parts. Section 2 describes briefly the computational techniques used in this study. The most relevant results obtained for the structural, electronic, mechanical and thermal properties for the compounds of interest are presented and discussed in Section 3. Finally, Section 4 summarizes the main conclusions.

2. Computational method

The geometry optimization, electronic structure, mechanical and thermodynamic properties calculations are performed within the full-potential linearized augmented plane wave (FP-LAPW) method [21]. The computational approach is based on the density functional theory (DFT) [22] implemented in WIEN2k package [23]. The exchange correlation potential is treated by Perdew-Burke-Ernzerhof (PBE-GGA) [24] and Wu-Cohen (WC-GGA)[25] approximations. The values of cutoff parameter $R_{MT}{*}K_{max} = 8.0$ and $l_{max} = 10$ are used to control the expansion of the partial waves inside the muffin-tin spheres. The muffin-tin radii (R_{MT}) are 2.1 (a.u) for transition atom (Sc, Y) and 2.3 (a.u) for Pt atom. The integral over Brillouin zone (IBZ) are performed with $10 \times 10 \times 10$ grids, using the Monkhort-Pack special *k*-points approach [26]. The iteration process is repeated until the calculated total energy of the crystal converges to less than 10^{-4} Ry. The valence electron configurations of Pt $4f^{14}5d^{9}6s$, Sc $3d^{4}s^{2}$ and Y $4d^{5}s^{2}$ are considered.

Table 1
Crystallographic data for $L1_2$, $D0_{22}$ and $D0_{24}$ structures.

Structure	*Proto-type*		*Space group (N°)*	*Wyckoff Position*
$L1_2$	Cu_3Au ($a = b = c$; $\alpha = \beta = \gamma = 90°$)		*Pm3m* (221)	Au (*1a*), Cu (*3c*)
$D0_{22}$	Al_3Ti ($a = b \neq c$; $\alpha = \beta = \gamma = 90°$)		*I4/mmm* (139)	Ti (*2a*), Al(*2b*), Al (*4d*)
$D0_{24}$	Ni_3Ti ($a = b \neq c$; $\alpha = \beta = 90°$; $\gamma = 120°$)		$P6_3/mmc$ (194)	Ti (*2a*), Ti (2c), Ni (*6g*), Ni(*6h*)

3. Results

3.1. Ground states properties

Most Pt_3TM compounds crystallize in the cubic $L1_2$, tetragonal $D0_{22}$and hexagonal $D0_{24}$ structures. In Table 1, the crystallographic data are listed for these structures. In order to determine the phase stability of Pt_3Sc and Pt_3Y compounds, we have calculated the total energy with respect to the unit cell volume for these structures. The obtained results agree well with the experimental data in the fact that for both compounds, the cubic $L1_2$ structure is the more stable one while the $D0_{24}$ structure is a meta stable (Fig. 1). The GGA total energy calculations difference between the $L1_2$ and $D0_{24}$ ($D0_{22}$) structures at equilibrium volume is around, in absolute value, 0.142 eV/atom (0.569 eV/atom) for Pt_3Sc compound and 0.145 eV/atom (0.162 eV/atom) for Pt_3Y compound. One can notice that for both compounds the values of $E(L1_2)$ and $E(D0_{24})$ are very close. The calculated total energies are fitted to the Murnaghan's equation of state [27]. The fit parameters (V_0, B, B′) and the available experimental and theoretical data are listed in Table 2 for both compounds in the stable phase. Table 2 shows that all obtained lattice parameters values are very close to the experimental measurement values and reveals that WC-GGA approximation performs well. Our computed structural values are in good agreement with previous theoretical ones [14,15]. Using the PBE-GGA scheme, the calculated formation enthalpies are −1.23 eV/atom and −1.18 eV/atom for Pt_3Sc and Pt_3Y which are close to the values of −1.06 eV/atom and −1.02 eV/atom for Pt_3Sc and Pt_3Y reported in Ref. [5], respectively.

3.2. Electronic properties

The total density of states (TDOS) calculations for Pt_3Sc and Pt_3Y compounds in the $L1_2$, $D0_{24}$ and $D0_{22}$ structures, using PBE-GGA approximation are shown in Fig. 2 (a, d) indicating that valence states extend from −8 to 8 eV. Also, the values of the TDOS at the Fermi level for both compounds are reported in Table 3. One can notice that for both

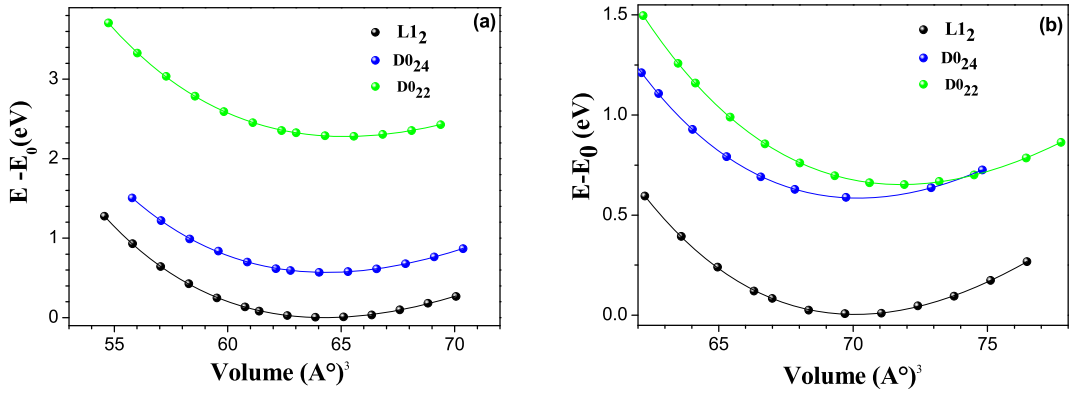

Fig. 1. Total energy versus volume per primitive cell of Pt_3Sc (a) and Pt_3Y (b), in the $L1_2$, $D0_{24}$ and $D0_{22}$ structures using PBE-GGA approximation. E_0 is the total energy of $L1_2$ phase at equilibrium for Pt_3Sc and Pt_3Y.

Table 2
Calculated and experimental lattice constants, volumes of unit cell V_0 and bulk modulus and its pressure derivative.

	V_0(Å^3)	a(Å)	B (GPa)	B′
Pt_3Sc				
PBE-GGA	64.29	4.006	195.63	5.00
WC-GGA	64.24	4.005	201.19	4.77
Exp [10]	62.00	3.958	–	–
Theo [14]	65.158	4.024	198.365	3.87
Theo [15]	64.908	4.019	205.27	5.8
Pt_3Y				
PBE-GGA	70.10	4.123	172.32	4.57
WC-GGA	67.51	4.072	193.75	4.62
Exp [11].	67.66	4.075		

Table 3
Total density of states at Fermi level $N_{tot}(E_f)$, for $L1_2$, $D0_{22}$ and $D0_{24}$ structures, density of states at Fermi level for Pt, Sc and Y atoms $N_{Pt/Sc/Y}$ (E_f), number of bonding electrons per atom n_b and the contribution of atomic orbital to binding, for $L1_2$ structure.

	$N_{tot}(E_f)$	$N_{Pt/Sc/Y}$ (E_f)	n_b
Pt_3Sc	3.22[a]($L1_2$),	Pt:0.83	n_b(Pt3Sc) = 8.24
	3.11[b]	Sc:0.12	n_b(Pt: 7.41; *s*: 0.34; *p*: 0.20;*d*:6.85)
	4.20[a]($D0_{24}$)		n_b (Sc = 0.98; *s*: 0.10; *p*: 0.15;*d*:0.72)
	4.77[a]($D0_{22}$)		
Pt_3Y	3.24[a]($L1_2$)	Pt:0. 83	n_b(Pt3Y) = 8.23
	3.75[a]($D0_{24}$),	Y:0.08	n_b(Pt = 7.42; *s*: 0.33; *p*: 0.16;*d*:6.90)
	4.67[a]($D0_{22}$)		n_b(Y = 0.76; *s*: 0.07; *p*: 0.20;*d*:0.46)

[a] this work.
[b] Ref. [14].

compounds, the value of the TDOS at Fermi level $N(E_F)$ for $L1_2$ structure is the lowest. These values show a clear inverse relationship with stability as confirmed by theory [28]. The TDOS falls down abruptly and reaches a minimum of 0.15 states/eV for $L1_2$ structure. The minimum of the TDOS is called pseudo-gap and is quite large (ΔE>1eV) and extends from approximately 0 to 2 eV, i. e this pseudo-gap resides between the binding and anti-binding regions. The electrons at the Fermi level are responsible for the electronic contribution in the heat capacity. This contribution is proportional to temperature and is very small and significant at low temperature ($C_{ele} = \gamma_{ele}T$). The electronic specific heat coefficient γ_{ele} is around 7.57 mJ mol^{-1}. K^{-2} for Pt_3Sc and 7.63 mJ mol^{-1}. K^{-2}for Pt_3Y. The electronic specific heat coefficient of pure platinum is 6.54 mJ mol^{-1}. K^{-2} as reported in Ref. [29]. The partial density of states (PDOS) shows that the (*d*) states are dominant for all atoms and the contribution of (*s, p*) states is very weak, for both compounds. At very low energy the (*s*) states are dominant, while around the Fermi level, the (*p*) states are dominant for all atoms (Fig. 2(d, c, e, f)).

The number of bonding electrons per atom (n_b) is 8.24 and 8.23 in the binding region for Pt_3Sc and Pt_3Y, respectively. Our value coincides with that reported by Chen 8.246 [15], for Pt_3Sc. In Table 3, the values of the orbital contribution to the binding are listed. According to these values, it is clearly seen that the contribution of the *d* states is larger for all atoms. If the (*s*) and (*p*) contributions are compared, we can notice that for Pt the (*s*) contribution is bigger than that of (*p*) and the inverse for the transition metal (Sc, Y). Therefore, the pseudo-gap indicates the strong *spd* hybridization and directing covalent bonding as for ordered intermetallic compounds [31–33].

To illustrate the bonding mechanism in these compounds, we have

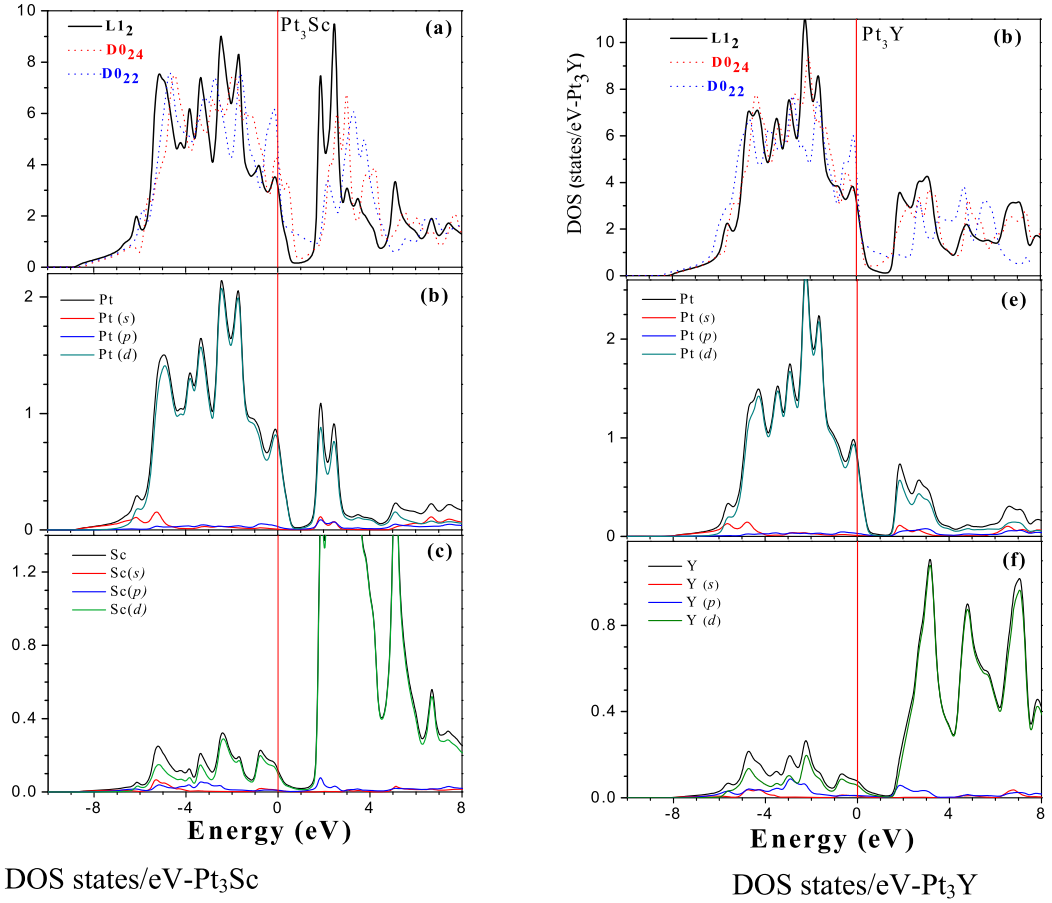

Fig. 2. Total densities of states of Pt_3Sc(a) and Pt_3Y (d) in $L1_2$, $D0_{24}$ and $D0_{22}$ structures, partial densities of states ofPt (c) and Sc(d) for Pt_3Sc and Pt (e) and Y(f) for Pt_3Y, in $L1_2$ structure.

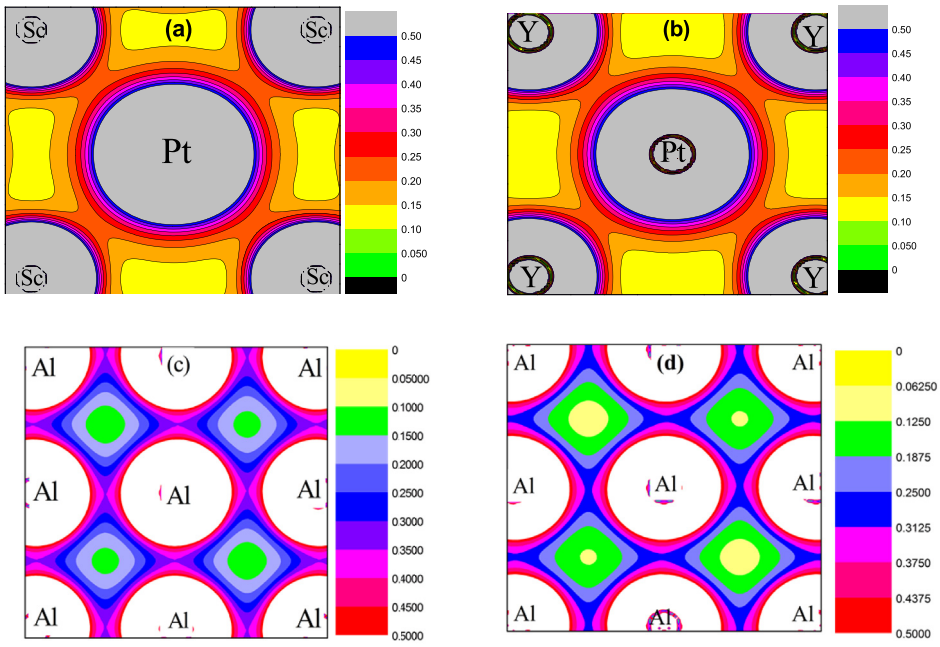

Fig. 3. Contour plot of the charge density of Pt_3Sc(a) and Pt_3Y(b) at plane (z = 0) and at z = 0.5 for Pt_3Sc(c) and Pt_3Y(d), in the $L1_2$ structure.

calculated the distribution of the electronic charge density in the elementary cell for the considered compounds in their stable phase $L1_2$ structure. Jahnátek et al. [31] identified two types of covalent bonds for this structure. Fig. 3 (a, b) show plots of the valence charge density distribution along (110) plane. We observe a depletion of the electronic charge at the lattice site, a build-up of electrons in the interstitial region and an overlapping electron distribution between Sc (Y) and Pt atoms which cause the bonds to be directed from Sc (Y) atoms to Pt atoms. The values of charge density, at midway between atoms, are 0.22 e/Å^2 for Pt_3Scand 0.23 e/Å^2 for Pt_3Y. The second type of bonds is that formed between Pt atoms only in the plane z = 0.5 (see Fig. 3(c and d)) where the charge is similarly distributed between 1st neighbour atoms.

3.3. Mechanical properties

The mechanical parameters of Pt_3Sc and Pt_3Y compounds are determined taking the advantage of calculating the elastic constants (C_{ij}). For the cubic $L1_2$ structure, there are only three independent elastic constants C_{11}, C_{12} and C_{44} [33]. Our calculated elastic constants satisfy the mechanical stab1ility criteria for a cubic crystal [34], which confirms the phase stability of these compounds. The Voigt-Reuss-Hill approximation is used to determine the shear modulus G_H [35]. The G_H (rigidity modulus) representing the resistance to plastic deformation is expressed as the average value $G_H = \frac{G_V+G_R}{2}$ of the Voigt's shear modulus $G_V = \frac{C_{11}-C_{12}+3C_{44}}{5}$ [36] and the Reuss's shear modulus $G_R = \frac{5C_{44}(C_{11}-C_{12})}{4C_{44}+3(C_{11}-C_{12})}$ [37]. The Young's modulus E and the Poisson ratio ν and anisotropy factor A are defined as

$$E = \frac{9BG_H}{3B + G_H}$$

$$\nu = \frac{3B - 2G}{2(3B + 3G)}$$

$$A = \frac{2C_{44}}{C_{11} - C_{12}}$$

The values of these constants and the elastic parameters are given in Table 4 compared with the available theoretical results. Table 4 shows

Table 4
Calculated elastic constants (GPa), elastic moduli (GPa), B/G ratio, Poisson's ratios, Debye Temperature (K) and anisotropic index of Pt_3Sc and Pt_3Y compounds, using PBE-GGA and WC-GGA.

Compounds	C_{11}	C_{12}	C_{44}	B	G_H	E	B/G	ν	A	θ_D
Pt_3Sc	292.2[a]	155.3[a]	110.6[a]	200.9[a]	91.2[a]	237.7[a]	2.20[a]	0.30[a]	1.61[a]	312.05[a]
	289.9[b]	147.7[b]	115.5[b]	195.1[b]	95.1[b]	245.4[b]	2.05[b]	0.29[b]	1.62[b]	318.09[b]
	379.4[c]	206.9[c]	89.1[c]	246.2[c]	74.7[c]	203.6[c]	G/B = 0.3[c]	0.36[c]	0.93[c]	–
	350.3[d]	194.1[d]	72.6[d]	292[d]	–	–	–	–	–	–
	286.58[e]	154.27[e]	113.91[e]	221.2[e]	94.798[e]	245.31[e]	–	0.294[e]	1.722[e]	398.70[e]
	290.74[f]	162.256[f]	111.77[f]	205.08[f]	61.077[f]	89.506[f]	–	–	–	–
Pt_3Y	243.4[a]	135.2[a]	86.7[a]	171.3[a]	71.7[a]	188.9[a]	2.39[a]	0.316[a]	1.60[a]	271.95[a]
	283.1[b]	157.6[b]	100.4[b]	199.5[b]	83.1[b]	218.9[b]	2.40[b]	0.317[b]	1.60[b]	290.94[b]

[a] This work (BPE-GGA).
[b] This work (WC-GGA).
[c] Ref. [12](LDA).
[d] Ref. [12](GGA).
[e] Ref. [14]PBE-GGA.
[f] Ref. [15] PBE-GGA.

Table 5
Sound velocities (in $m.s^{-1}$), Debye temperature (in K) and melting temperature (in K) of the Pt_3Sc and Pt_3Ycompounds, using PBE-GGA and WC-GGA.

Compounds	ν_t	ν_l	ν_m	Θ_D	$T_m \pm 300$
Pt_3Sc	2367.22[a]	4451.5	2645.09	312.053	2279.6242
	2416.22[b]	4445.55	2695.6	318.091	2266.6831
				398.700[c]	1850 (C)[d]
Pt_3Y	2119.62[a]	4088.22	2372.48	271.95	1991.5424
	2239.33[c]	4326.36	2506.75	290.939	2226.2315

[a] This work(BPE-GGA).
[b] This work (WC-GGA).
[c] Ref. [14](BPE-GGA).
[d] Ref. [45](Exp.).

that the calculated value of the bulk modulus B, which describes the resistance to fracture, from the elastic constants $B = (C_{11}+2C_{12})/3$ is close to the value obtained from the total energy calculation. The Young's modulus is often related to the stiffness of the material. Large values of Young's modulus indicate that the material is stiffer [38]. The Pt_3Sc Young's modulus value is larger than that of Pt_3Y; therefore, Pt_3Sc is stiffer than Pt_3Y compound. Pugh [39] reported that the high and low value of B/G ratio is related to the ductility and brittleness of materials, respectively. From Table 4, we can say that Pt_3Sc and Pt_3Y compounds are ductile because the values of B/G ratios are larger than 1.75 (1.75: critical value of B/G separates the ductile and brittle limit). This ductility is confirmed by the value of the positive Cauchy pressure (C_{12}–C_{44}). Pettifor [40] suggested that if the Cauchy pressure (C_{12}–C_{44}) is positive (negative) the material is expected to be ductile (brittle). The ductility or brittleness materials are interpreted by Poisson ratio as well. The values of Poisson's ratio for covalent, ionic, and metallic materials are 0.1, 0.25 and 0.33, respectively [41]. Herein, the value of

Table 6
Selection of thermal properties at 300 K: isothermal and adiabatic bulk moduli (B and B_S, in GPa), heat capacities (Cv and Cp in J/mol. K), thermal expansion coefficient (α, 10^{-5}/K), Debye temperature (θ_D, K) and Grüneisen parameter (γ).

Compounds	B	B_s	C_v	C_p	α	θ_D	γ
Pt_3Sc	161.30	170.04	94.05	99.16	5.18	328.01	3.490
Pt_3Y	153.40	158.33	94.50	97.54	3.93	314.30	2.724

Poisson ratio is found to be equal to 0.30 for Pt_3Sc and 0.31 for Pt_3Y, which indicates that our compounds possess a metallic behavior and are both ductile. For isotropic crystals, the value of A is equal to unity and any deviation from unity indicates anisotropy [42]. Our calculations reveal that all calculated anisotropy factor differ from unity. This indicates that the studied compounds are anisotropic. In comparison with theoretical results reported in literature, we notice that our results are in good agreement with those reported in Refs. [14,15] for Pt_3Sc. However for Pt_3Y, to the best of our knowledge, there are no available data in literature. Hence, our results are original and can serve as reference data for future works.

One of the standard methods to calculate the Debye temperature is that from the elastic constants data [43]

$$\theta_D = \frac{h}{k_B}\left[\frac{3n}{4\pi}\left(\frac{N_A\rho}{M}\right)\right]^{1/3}\nu_m$$

where $\nu_m = \left[\frac{1}{3}\left(\frac{2}{\nu_t^3}+\frac{1}{\nu_l^3}\right)\right]^{-1/3}$, $\nu_t = \left(\frac{G}{\rho}\right)^{1/2}$, $\nu_l = \left(\frac{3B+4G}{3\rho}\right)^{1/2}$

Here h is Planck's constant, k_B is Boltzmann's constant, N_A is Avogadro's number, ρ is the mass density, M is the molar mass per unit cell, n is the number of atoms per unit cell and ν_m, ν_t and ν_l are the average,

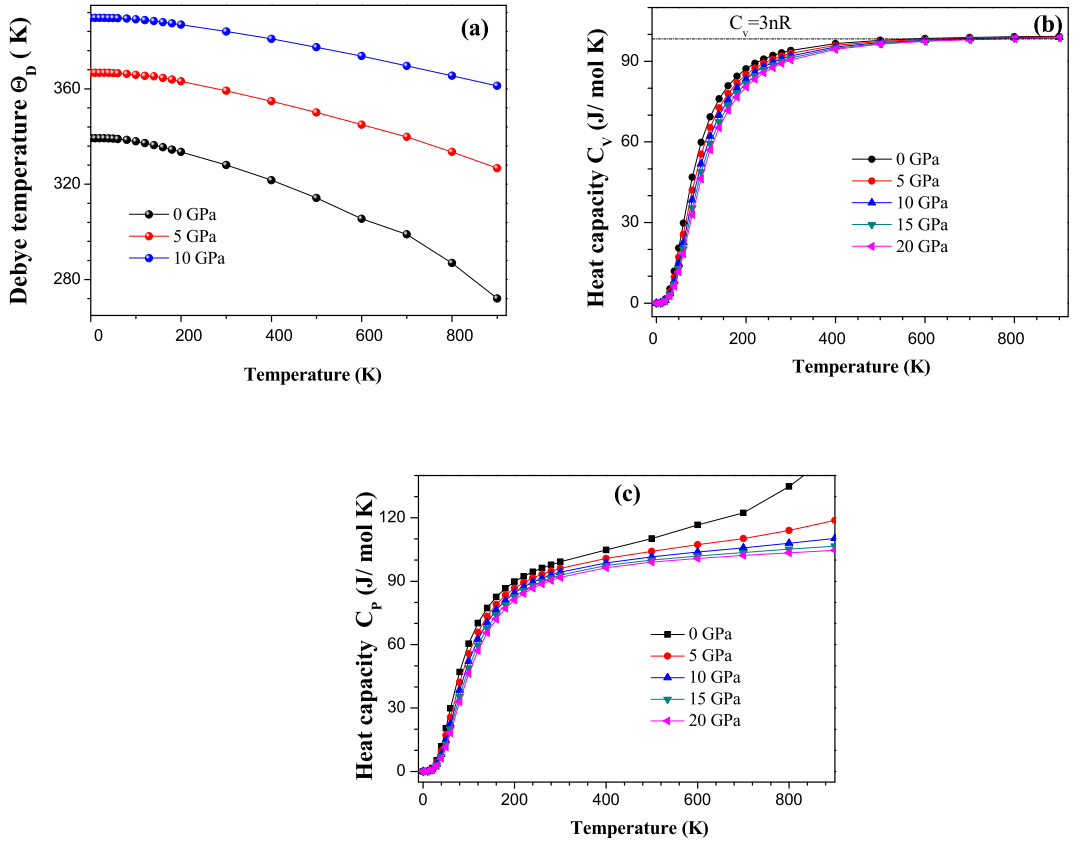

Fig. 4. Thermal properties vs temperature at various pressures. Debye Temperature (a) and heat capacities C_V (b) and C_p (c) for Pt_3Sc compound, because of similarity and simplicity, the Pt_3Y curves are not given.

transverse and longitudinal sound velocities, respectively. In addition, the melting temperatures of the considered materials are determined using the empirical relation [44]:

$$T_m = [553K + (5.91K/GPa)C_{11}] \pm 300K$$

The obtained values for Pt_3Sc and Pt_3Y are reported in Table 5. To the best of our knowledge, there are no experimental and other theoretical data for comparison. Our computed value of Θ_D, for Pt_3Sc, is less than that reported by Arikan et al. [14], however, it coincides well with that extracted data from the curve of Θ_D (T) reported in Ref. [15]. Moreover, the melting point for Pt_3Sc is in good agreement with the experimental data [45].

3.4. Thermal properties

To determine the thermodynamic properties of the compounds, we apply the quasi-harmonic Debye model implemented in the GIBBS program [46]. This program uses the total energy as a function of the molecular volume (V) to generate the Debye temperature θ_D (V) and the minimization of the non-equilibrium Gibbs function G*(V; P, T). It gives the effect of the pressure (P) and temperature (T) on the volume of unit cell, bulk modulus, heat capacities (Cv and Cp) thermal expansion coefficient (α), Debye temperature θ_D ….etc. This procedure is described in details in Ref. [46]. The thermal properties are determined in a temperature range from 0 to 900 K, where the quasi-harmonic model remains completely valid. The pressure effect is studied in the 0–20 GPa range. Table 6 reports the values, at ambient conditions (P = 0 GPa, T = 300 K), of the isothermal and adiabatic bulk moduli (B and B_S), heat capacities (Cv and Cp), thermal expansion coefficient (α), Debye temperature (θ_D) and Grüneisen parameter (γ). In the study of the material thermodynamic properties, it is very important to determine θ_D which is correlated with many physical properties such as melting temperature, specific heat and elastic constants. Fig. 4(a) shows the variation of θ_D with respect to temperature, where we observe that at very low temperatures (T < 70 K) θ_D is quite constant, and diminishes quite linearly for T > 70 K. At fixed temperature, θ_D increases with pressure and the temperature effect becomes less significant with pressure. In the previous section, we calculated θ_D from elastic constants (see Table 4); the values are close to those obtained from quasi-harmonic Debye model (see Table 5). Rajagopalan et al., using first principles calculations, reported 244.15 K for Pt_3V Debye temperature value [47] and 334.3 K for Ti_3Pt [48]. In the Debye model, the adiabatic bulk modulus is close to the isothermal bulk modulus ($B_s \approx B$), whereas these values are lower than that obtained with volume optimization curves. The heat capacity is an important parameter that characterizes the thermal properties of solids. It is the energy required to change the temperature of the solid by 1 K. The energy variation with temperature gives us C_v at constant volume, and C_p at constant pressure. Fig. 4 (b and c) show the variation of heat capacities C_v and C_p with respect to temperature at pressures: 0, 5, 10, 15 and 20 GPa. It is clearly seen that C_v follows the Debye law [49]. At low temperature (T < 500 K), C_v is proportional to T^3 and decreases with pressure. At higher temperatures (T > 500 K), the anharmonic and pressure effects on the heat capacity C_v are negligible and C_v is close to the classical Dulong-Petit limit [50] ($C_v = 3R = 25$ J/mol. K, for mono-atomic solid). Furthermore, C_p continues to increase with temperature and decreases with pressure. At low temperatures, C_p has the same behavior of C_v. At very low temperatures (T < 70 K), both C_v and C_p vary slightly with temperature and pressure.

4. Conclusion

First principles method was used to study the structural, elastic, electronic and thermodynamic properties for the intermetallic compounds Pt_3Sc and Pt_3Y. The total energy calculations show that the $L1_2$ structure is the more stable one, compared to the $D0_{22}$, and $D0_{24}$ structures. The ground state properties like enthalpies of formation, lattice constants and bulk modulus and its pressure derivative are calculated and compared. The densities of states (DOS) calculations show the existence of a pseudo-gap near the Fermi level. This pseudo-gap indicates the strong *spd* hybridization and directing covalent bonding. The density of states at Fermi level $N(E_F)$, the electronic specific heat coefficient (γ_{ele}) and the number of bonding electrons per atom are estimated. The elastic constants (C_{11}, C_{12} and C_{44}) are determined. The shear modulus (G_H), Young's modulus (E), Poisson's ratio (ν), anisotropy factor (A), ratio of B/G_H and Cauchy pressure (C_{12}–C_{44}) are also estimated. These parameters show that the Pt_3Sc and Pt_3Y possess a metallic behavior and are both ductile. Hence, we can state that the inter-atomic bonding is a mixture of the covalent and metallic bonding. The Debye temperature is estimated from the average sound velocity. Finally, the quasi harmonic Debye model is successfully used to predict the thermodynamic properties in the whole pressure range from 0 to 20 GPa and temperature range from 0 K to 900 K. Our calculated parameter values are in good agreement with available results reported in literature for Pt_3Sc compound which validates our results. Finally, it is worth noting that for Pt_3Y compound almost all of the parameters are newly investigated in this work.

References

[1] C.T. Liu, I. Baker, R. Darolia, J.D. Whittenberger, M.H. Yoo (Eds.), MRS Symp. Proc., VoI. 288, 1993, p. 3. Pittsburgh, PA.
[2] M.H. Yoo, S.L. Sass, C.L. Fu, M.J. Mills, D.M. Dimiduk, E.P. George, Acta Metall. Mater. 41 (1993) 87.
[3] C.T. Sims, N.S. Stoloff, W.C. Hagel, Superalloy II, John Wiley and Sons, New York, 1987.
[4] Q. Feng, T.K. Nandy, S. Tin, T.M. Pollock, Acta Mater. 51 (2003) 269.
[5] J. Greeley, I.E.L. Stephens, A.S. Bondarenko, T.P. Johansson, H.A. Hansen, T.F. Jaramillo, J. Rossmeisl, I. Chorkendorff, J.K. Nørskov, Nat. Chem. 1 (2009) 552.
[6] U. Bardi, D. Dahlgren, P.N. Ross, J. Catal. 100 (1986) 196.
[7] L. Meddar, S. Garbarino, M. Danaie, G.A. Botton, D. Guay, Thin Solid Films 524 (2012) 127.
[8] G.H. Jóhannesson, T. Bligaard, A.V. Ruban, H.L. Skriver, K.W. Jacobsen, J.K. Nørskov, Phys. Rev. Lett. 88 (2002) 255506-1–255506-5.
[9] Qiti Guo, O.J. Kleppa, J. Alloy. Comp. 321 (2001) 169.
[10] A.E. Dwight, R.A. Conner Jr., Acta Crystallogr. 14 (1961) 75.
[11] A.E. Dwight, R.A. Conner jr, J.W. Downey, Acta Crystallogr. 18 (1965) 837.
[12] V.I. Razumovskiya, E.I. Isaevb, A.V. Ruban, P.A. Korzhavyi, Intermetallics 16 (2008) 982.
[13] L.V. Goncharuk, V.R. Sidorko, V.G. Khoruzhaya, T.Y. Velikanova, Powder Metall. Met. Ceram 39 (1–2) (2000) 55.
[14] N. Arikan, A. Iyigor, A. Candan, S. Ugur, Z. Charifi, H. Baaziz, G. Ugur, Comput. Mater. Sci. 79 (2013) 703.
[15] Bao Chen, Santao Qi, Hongquan Song, Chuanhui Zhang, Jiang Shen, Mod, Phys. Lett. B 29 (32) (2015) 1550201.
[16] P. Giannozzi, et al., J. Phys. Condens. Matter 21 (39) (2009) 395502.
[17] M. Sundareswari, M. Rajagopalan, Eur. Phys. J. B 49 (1) (2006) 67.
[18] T. Jeong, Solid State Commun. 140 (6) (2006) 304.
[19] S. Gao, Comput. Phys. Commun. 153 (2003) 190.
[20] K. Schwarz, J. Solid State Chem. 176 (2003) 319.
[21] O.K. Anderson, Phys. Rev. B 42 (1975) 3060.
[22] P. Hohenberg, W. Kohn, Phys. Rev. B 136 (1964) 864.
[23] P. Blaha, K. Schwarz, G.K.H. Madsen, D. Kvasnicka, J. Luitz, WIEN2k, an Augmented Plane Wave Plus Local Orbitals Program for Calculating Crystal Properties, Vienna University of Technology, Vienna, Austria, 2001.
[24] J.P. Perdew, K. Burke, M. Ernzerhof, Phys. Rev. Lett. 77 (1996) 3865.
[25] Z. Wu, R.E. Cohen, Phys. Rev. B 73 (2006) 235116.
[26] H.J. Monkhorst, J.D. Pack, Phys. Rev. B 13 (1976) 5188.
[27] F.D. Murnaghan, Proc. Natl. Acad. Sci. U.S.A. 30 (1944) 244.
[28] J.H. Xu, T. Oguchi, A.J. Freeman, Phys. Rev. B 36 (1987) 4186.
[29] G.R. Stewart, Rev. Sci. Instrum. 54 (1) (1983) 1.
[31] M. Jahnátek, M. Krajčí, J. Hafner, Phys. Rev. B 71 (2005) 024101.
[32] T. Hong, T.J. Watson-Yang, A.J. Freeman, Phys. Rev. B 41 (1990) 12462.
[33] M.J. Mehl, B.M. Klein, K. Papaconstantapolous, Intermetallic Compounds, John Wiely& Sons, New York, 1994.
[34] J. Wang, S. Yip, Phys. Rev. Lett. 71 (1993) 4182.
[35] R. Hill, Proc. Phys. Soc., London 65 (1952) 349.
[36] W. Voigt, Ann. Phys. 38 (1889) 573.
[37] A. Reuss, Z. Angew, Math. Phys. 9 (1929) 49.
[38] C.H. Jenkins, S.K. Khanna, Mech. Mater. (2005) 62.
[39] S.F. Pugh, Philos. Mag. A 45 (1954) 823.
[40] D.G. Pettifor, Mater. Sci. Technol. 8 (1992) 345.
[41] J. Haines, J. Léger, G. Bocquillon, Annu. Rev. Mater. Sci. 31 (2001) 1.
[42] R.E. Newnham, Properties of Materials; Anisotropy, Symmetry, Structure, Oxford University Press, New York, NY, USA, 2005.

[43] O.L. Anderson, J. Phys. Chem. Solids 24 (1963) 909.
[44] C. Nianyi, L. Chonghe, Y. Shuwen, W. Xueye, J. Alloy. Comp. 234 (1996) 130.
[45] T.B. Massalski, Binary Alloy Phase Diagrams, second ed., vol. 3, ASTM International, Materials Park,Ohio, 1990, p. 3125.
[46] M.A. Blanco, E. Francisco, V. Luaña, Comput. Phys. Commun. 158 (2004) 57.
[47] M. Rajagopalan, Physica B 405 (2010) 2516.
[48] M. Rajagopalan, R. Rajiv Gandhi, Physica B 407 (2012) 4731.
[49] P. Debye, Ann. Phys. 39 (1912) 789.
[50] A.T. Petit, P.L. Dulong, Ann. Chim. Phys. 10 (1819) 395.